One- and three-photon dynamical Casimir effects using a nonstationary cyclic qutrit

H. Dessano[1,2] and A. V. Dodonov[1,3,*]

[1]*Institute of Physics, University of Brasilia, 70910-900 Brasilia, Federal District, Brazil*

[2]*Instituto Federal de Brasília, Campus Recanto das Emas, 72620-100 Brasilia, Federal District, Brazil*

[3]*International Centre for Condensed Matter Physics, University of Brasilia, 70910-900 Brasilia, Federal District, Brazil*

(Received 13 May 2018; published 31 August 2018)

We consider a nonstationary circuit quantum electrodynamics setup in which a three-level artificial atom in the Δ configuration interacts with a single-mode cavity field of natural frequency ω. It is demonstrated that when some atomic energy level(s) undergoes a weak harmonic modulation, photons can be generated from vacuum via effective one- and three-photon transitions, while the atom remains approximately in the ground state. These phenomena occur in the dispersive regime when the modulation frequency is accurately tuned near ω and 3ω, respectively, and the generated field states exhibit strikingly different statistics from the squeezed vacuum state attained in the standard cavity dynamical Casimir effect.

DOI: 10.1103/PhysRevA.98.022520

I. INTRODUCTION

The term *cavity dynamical Casimir effect* (DCE) can be used to denote the class of phenomena that feature the generation of photons from vacuum in some cavity due to the resonant external perturbation of the system parameters, where the cavity serves to produce a resonant enhancement of the DCE [1–6]. These phenomena were originally studied in the context of electromagnetic resonators with oscillating walls or containing a macroscopic dielectric medium with time-modulated internal properties [7–12] but were later generalized for other bosonic fields, e.g., phononic excitations of ion chains [13], optomechanical systems [14], cold atoms [15], and Bose-Einstein condensates [16,17]. For single-mode cavities the main resonance occurs near the modulation frequency 2ω, where ω is the bare cavity frequency, and in the absence of dissipation the average photon number increases exponentially with time [18,19], resulting in a squeezed vacuum state with even photon numbers, analogously to the phenomenon of parametric amplification [1,4,9]. The cavity DCE was recently implemented experimentally using a Josephson metamaterial consisting of an array of 250 superconductive interference devices (SQUIDs) embedded in a microwave cavity whose electrical length was modulated by an external magnetic flux [20].

The concept of the cavity DCE has been successfully extended to the area of circuit quantum electrodynamics (QED) [21–24], in which one or several artificial Josephson atoms strongly interact with a microwave field confined in superconducting resonators and waveguides [25–28]. The exquisite *in situ* control over the atomic parameters allows us to rapidly modulate the atomic energy levels and the atom-field coupling strength [29–35], enabling the use of artificial atoms as substitutes of the dielectric medium with time-dependent properties. From the viewpoint of a toy model [36], a modulated or oscillating dielectric slab can be imagined as a set of atoms with varying parameters, so ultimately the DCE must emerge for a single nonstationary two-level atom. Indeed, it was shown that for an off-resonant qubit(s) undergoing a weak external perturbation, pairs of photons are generated from vacuum under the modulation frequency $\sim 2\omega$ while the atom(s) remains approximately in the initial state [21,24,36,37]. In this scenario the atom plays the role of both the source and the real-time detector of DCE, since the (low) atomic transition probability depends on the photon number and in turn affects the photon generation pattern [21,38,39]. Moreover, the rich nonharmonic spectrum of the composite atom-field system permits the implementation of other phenomena in the nonstationary regime, such as sideband transitions [40–42], the antidynamical Casimir effect [36,39,43–45], the n-photon Rabi model [46], generation of entanglement [47,48], quantum simulations [32,49,50], and the dynamical Lamb effect [51,52].

Here we explore theoretically the prospects of implementing nontraditional versions of cavity DCE using three-level atoms (qutrits) in the cyclic (also known as the Δ) configuration subject to parametric modulation. In this case all the transitions between atomic levels can occur simultaneously via the cavity field [53–56], so the total number of excitations is not conserved even upon neglecting the counter-rotating terms (CRTs; rotating-wave approximation). Although prohibited by the electric-dipole selection rules for usual atoms, the Δ configuration can be implemented for certain artificial atoms in circuit QED [28] by breaking the inversion symmetry of the potential energy. Our goal is to find new modulation frequencies, exclusive of the cyclic qutrits, that induce photon generation from vacuum without appreciably changing the atomic state.

We find that for the harmonic modulation of some energy level(s) of a dispersive cyclic qutrit, photons can be generated from vacuum for the modulation frequencies $\eta \approx \omega$ and $\eta \approx 3\omega$, while the atom predominantly remains in the ground state. We call these processes one- and three-photon DCE because

*adodonov@fis.unb.br

the photons are generated via effective one- and three-photon transitions between the system's dressed states, whose rates depend on the product of all three coupling strengths. We derive an approximate analytical description of the unitary dynamics and illustrate the typical system behavior by solving numerically the Schrödinger equation. In particular, we show that the average photon number and atomic populations display a collapse-revival behavior, and the photon number distributions are completely different from the standard (two-photon) cavity DCE case. Moreover, we solve numerically the Markovian master equation and demonstrate that in the presence of weak dissipation the dissipative dynamics resembles the unitary one at initial times, confirming that our proposal is experimentally feasible.

II. PHYSICAL SYSTEM

We consider a single cavity mode of constant frequency ω that interacts with a qutrit in the cyclic configuration [28,53–56], so that all atomic transitions are allowed via one-photon transitions. The Hamiltonian reads

$$\hat{H}/\hbar = \omega\hat{n} + \sum_{k=1}^{2} E_k(t)\hat{\sigma}_{k,k} + \sum_{k=0}^{1}\sum_{l>k}^{2} g_{k,l}(\hat{a}+\hat{a}^\dagger)(\hat{\sigma}_{l,k}+\hat{\sigma}_{k,l}). \quad (1)$$

$\hat{a}$ ($\hat{a}^\dagger$) is the cavity annihilation (creation) operator and $\hat{n} = \hat{a}^\dagger\hat{a}$ is the photon number operator. The atomic eigenenergies are $E_0 \equiv 0$, E_1, and E_2, the corresponding states are $|\mathbf{k}\rangle$, and we define $\hat{\sigma}_{k,j} \equiv |\mathbf{k}\rangle\langle\mathbf{j}|$. The constant parameters $g_{k,l}$ denote the coupling strengths between the atomic states $|\mathbf{k}\rangle$ and $|\mathbf{l}\rangle$ mediated by the cavity field. To emphasize the role of the counter-rotating terms we rewrite (for $l > k$)

$$g_{k,l}(\hat{a}+\hat{a}^\dagger)(\hat{\sigma}_{l,k}+\hat{\sigma}_{k,l}) \to g_{k,l}(\hat{a}\hat{\sigma}_{l,k} + c_{k,l}\hat{a}\hat{\sigma}_{k,l} + \text{H.c.}),$$

where $c_{k,l} = 1$ when the corresponding CRT is taken into account and is $c_{k,l} = 0$ otherwise.

Utilizing the tunability of Josephson atoms [29–35], we assume that the atomic energy levels can be modulated externally as

$$E_k(t) \equiv E_k^{(0)} + \varepsilon_k \sin(\eta t + \phi_k) \quad \text{for} \quad k = 1, 2,$$

where $\varepsilon_k \ll E_k^{(0)}$ is the modulation amplitude, ϕ_k is the associated phase, $E_k^{(0)}$ is the bare energy value, and $\eta \gtrsim \omega$ is the modulation frequency. We would like to stress that for weak perturbations our approach can be easily generalized to multitone modulations or simultaneous perturbation of all the parameters in Hamiltonian (1).

We expand the wave function as

$$|\psi(t)\rangle = \sum_{n=0}^{\infty} e^{-it\lambda_n} b_n(t)\mathcal{F}_n(t)|\varphi_n\rangle,$$

$$\mathcal{F}_n(t) = \exp\left\{\sum_{k=1}^{2}\frac{i\varepsilon_k}{\eta}[\cos(\eta t+\phi_k)-1]\langle\varphi_n|\hat{\sigma}_{k,k}|\varphi_n\rangle\right\}. \quad (2)$$

Here λ_n are the eigenfrequencies of the bare Hamiltonian $\hat{H}_0 \equiv \hat{H}$ [$\varepsilon_1 = \varepsilon_2 = 0$] ($n$ increasing with energy) and $|\varphi_n\rangle$ are the corresponding eigenstates (dressed states). $b_n(t)$ denotes the slowly varying probability amplitude of the state $|\varphi_n\rangle$ and $\mathcal{F}_n(t) \approx 1$ is a rapidly oscillating function with a low amplitude.

After substituting Eq. (2) into the Schrödinger equation, to first order in ε_1 and ε_2 we obtain the differential equation

$$\dot{b}_n = \sum_{m\neq n} b_m[\Theta^*_{m;n}e^{it(\lambda_n-\lambda_m-\eta)} - \Theta_{n;m}e^{-it(\lambda_m-\lambda_n-\eta)}], \quad (3)$$

which describes transitions between the dressed states $|\varphi_n\rangle$ and $|\varphi_m\rangle$ at the transition rate $|\Theta_{n;m}|$, where

$$\Theta_{n;m} \equiv \frac{1}{2}\sum_{k=1}^{2}\varepsilon_k e^{i\phi_k}\langle\varphi_n|\hat{\sigma}_{k,k}|\varphi_m\rangle. \quad (4)$$

The transition $|\varphi_n\rangle \leftrightarrow |\varphi_m\rangle$ occurs when the modulation frequency is resonantly tuned to $\eta_r = |\lambda_m - \lambda_n| + \Delta\nu$, where $\Delta\nu$ denotes a small shift [24] dependent on $\varepsilon_1, \varepsilon_2$ due to the rapidly oscillating terms that were neglected in Eq. (3) (in this paper we adjust $\Delta\nu$ numerically). By writing the interaction-picture wave function as $|\psi_I(t)\rangle = \sum_n b_n(t)|\varphi_n\rangle$ one can cast Eq. (3) as a dressed-picture *effective Hamiltonian*,

$$\hat{H}_{\text{ef}}(t) = -i\sum_{n,m\neq n}\Theta_{m;n}|\varphi_m\rangle\langle\varphi_n|e^{-it(\lambda_n-\lambda_m-\eta)} + \text{H.c.}$$

Since we focus on transitions in which the atom is minimally disturbed, we consider the dispersive regime

$$|\Delta_1|, |\Delta_2|, |\Delta_1+\Delta_2| \gg \sqrt{n_{\max}}\max(g_{k,l}),$$

where $n_{\max}$ is the maximum number of system excitations and the bare detunings are defined as

$$\Delta_1 \equiv \omega - E_1^{(0)}, \quad \Delta_2 \equiv \omega - \left(E_2^{(0)} - E_1^{(0)}\right),$$
$$\Delta_3 \equiv \Delta_1 + \Delta_2.$$

Denoting by $|\zeta_k\rangle$ the dressed states in which the atom is predominantly in the ground state, from the standard perturbation theory we find

$$|\zeta_k\rangle \approx |\mathbf{0},k\rangle + \frac{c_{0,1}g_{0,1}^2\sqrt{k(k-1)}}{2\Delta_1\omega}|\mathbf{0},k-2\rangle + \frac{g_{0,1}\sqrt{k}}{\Delta_1}|\mathbf{1},k-1\rangle - \frac{c_{0,1}g_{0,1}\sqrt{k+1}}{2\omega-\Delta_1}|\mathbf{1},k+1\rangle - \frac{c_{1,2}g_{0,1}g_{1,2}k}{\Delta_1(2\omega-\Delta_3)}|\mathbf{2},k\rangle + \frac{g_{0,1}g_{1,2}\sqrt{k(k-1)}}{\Delta_1\Delta_3}|\mathbf{2},k-2\rangle - \frac{g_{0,2}\sqrt{k}}{\omega-\Delta_3}|\mathbf{2},k-1\rangle - \frac{c_{0,2}g_{0,2}\sqrt{k+1}}{3\omega-\Delta_3}|\mathbf{2},k+1\rangle, \quad (5)$$

where $|\mathbf{j},k\rangle \equiv |\mathbf{j}\rangle_{\text{atom}} \otimes |k\rangle_{\text{field}}$ and $k \geqslant 0$. The corresponding eigenfrequencies are (neglecting constant shifts)

$$\Lambda_k \approx \omega_{\text{ef}}k + \alpha k^2, \quad (6)$$

with the effective cavity frequency and the one-photon Kerr nonlinearity, respectively,

$$\omega_{\rm ef} \equiv \omega + \frac{g_{0,1}^2}{\Delta_1}\left(1 - \frac{g_{1,2}^2}{\Delta_1\Delta_3}\right) - \frac{g_{0,2}^2}{\omega - \Delta_3} - \frac{c_{0,1}g_{0,1}^2}{2\omega - \Delta_1} - \frac{c_{0,2}g_{0,2}^2}{3\omega - \Delta_3},$$

$$\alpha \equiv \frac{g_{0,1}^2}{\Delta_1^2}\left(\frac{g_{1,2}^2}{\Delta_3} - \frac{g_{0,1}^2}{\Delta_1} + \frac{c_{0,1}g_{0,1}^2}{2\omega} - \frac{c_{1,2}g_{1,2}^2}{2\omega - \Delta_3} + \frac{g_{0,2}^2}{\omega - \Delta_3} + \frac{c_{0,1}g_{0,1}^2}{2\omega - \Delta_1} + \frac{c_{0,2}g_{0,2}^2}{3\omega - \Delta_3}\right).$$

In the Appendix we present the complete expressions for the eigenstates and eigenvalues obtained from the second- and fourth-order perturbation theory, respectively.

III. ONE- AND THREE-PHOTON DCE

The lowest-order phenomena that occur exclusively for cyclic qutrits depend on the combination $g_{0,1}g_{1,2}g_{0,2}$, so we define $G^3 \equiv g_{0,1}g_{1,2}g_{0,2}/2$. Indeed, for $g_{0,2} = 0$ we recover the ladder configuration, for $g_{0,1} = 0$ the Λ configuration, and for $g_{1,2} = 0$ the V configuration. After substituting the dressed states, (A1), into Eq. (4) we find that one such effect is the three-photon transition between the states $|\zeta_k\rangle$ and $|\zeta_{k+3}\rangle$. To lowest order the respective transition rate reads

$$\Theta_{k;k+3}^{(\zeta)} = G^3\sqrt{\frac{(k+3)!}{k!}}[\varepsilon_1 q_1 e^{i\phi_1} - \varepsilon_2 q_2 e^{i\phi_2}], \tag{7}$$

where the k-independent parameters are

$$q_1 = \frac{c_{0,2}}{\Delta_1(3\omega - \Delta_3)(3\omega - \Delta_1)} + \frac{c_{0,1}c_{1,2}}{(2\omega - \Delta_1)(\omega - \Delta_3)(\omega + \Delta_1)},$$

$$q_2 = \frac{c_{0,2}}{\Delta_1\Delta_3(3\omega - \Delta_3)} + \frac{c_{0,1}c_{1,2}}{(2\omega - \Delta_1)(\omega - \Delta_3)(4\omega - \Delta_3)}.$$

We see that this effect, corresponding roughly to the transitions $|\mathbf{0}, k\rangle \leftrightarrow |\mathbf{0}, k+3\rangle \leftrightarrow |\mathbf{0}, k+6\rangle \leftrightarrow \ldots$, relies on the CRT: either $c_{0,2}$ or the product $c_{0,1}c_{1,2}$ must be nonzero.

The second effect allowed by the cyclic configuration is the one-photon transition between the states $|\zeta_k\rangle$ and $|\zeta_{k+1}\rangle$ or, roughly, $|\mathbf{0}, k\rangle \leftrightarrow |\mathbf{0}, k+1\rangle \leftrightarrow |\mathbf{0}, k+2\rangle \leftrightarrow \ldots$. We obtain, to lowest order,

$$\Theta_{k;k+1}^{(\zeta)} = G^3\sqrt{k+1}[\varepsilon_1 Q_1(k)e^{i\phi_1} - \varepsilon_2 Q_2(k)e^{i\phi_2}], \tag{8}$$

where we have defined k-dependent functions

$$Q_1(k) = \frac{1}{\Delta_1(\omega - \Delta_1)}\left(\frac{c_{1,2}c_{0,2}(k+1)}{3\omega - \Delta_3} + \frac{k}{\omega - \Delta_3}\right) - \frac{c_{0,1}c_{0,2}(k+2)}{(2\omega - \Delta_1)(3\omega - \Delta_3)(3\omega - \Delta_1)} - \frac{c_{1,2}k}{\Delta_1(\omega - \Delta_3)(\omega + \Delta_1)} - \frac{c_{0,1}}{(\omega - \Delta_1)(2\omega - \Delta_1)} \times \left(\frac{c_{1,2}c_{0,2}(k+2)}{3\omega - \Delta_3} + \frac{k+1}{\omega - \Delta_3}\right),$$

$$Q_2(k) = \frac{1}{(2\omega - \Delta_3)(\omega - \Delta_3)}\left(\frac{c_{0,1}(k+1)}{2\omega - \Delta_1} - \frac{c_{1,2}k}{\Delta_1}\right) + \frac{c_{0,1}c_{1,2}c_{0,2}(k+2)}{(2\omega - \Delta_1)(4\omega - \Delta_3)(3\omega - \Delta_3)} + \frac{k}{\Delta_1\Delta_3(\omega - \Delta_3)} + \frac{c_{0,2}}{(2\omega - \Delta_3)(3\omega - \Delta_3)} \times \left(\frac{c_{0,1}(k+2)}{2\omega - \Delta_1} - \frac{c_{1,2}(k+1)}{\Delta_1}\right).$$

We see that for $k > 0$ (nonvacuum field states) the CRTs are not required for this effect, but for photon generation from vacuum either $c_{0,1}$ or the product $c_{1,2}c_{0,2}$ must be nonzero. In analogy to the generation of photon pairs in the standard DCE, we call the above effects the three- and one-photon DCE, respectively.

As seen from Eqs. (7) and (8), to induce the one- and three-photon DCE it is sufficient to modulate just one of the energy levels, yet the simultaneous modulation of both E_1 and E_2 can increase the transition rate provided the phase difference $(\phi_1 - \phi_2)$ is properly adjusted. However, for a constant modulation frequency the photon generation from vacuum is limited due to the resonance mismatch for multiphoton dressed states. Indeed, from Eq. (6) we have

$$\Lambda_{k+J} - \Lambda_k = (\omega_{\rm ef} + J\alpha)J + (2\alpha J)k,$$

where $J = 1, 3$. Assuming realistically that $g_{l,k}$ and ε_j are all of the same order of magnitude, we note that $|\alpha| \gtrsim |\Theta_{k;k+J}^{(\zeta)}|$ for $k \sim 1$. Hence for constant $\eta_J \simeq \Lambda_J - \Lambda_0$ (adjusted to generate photons from vacuum) the coupling between the states $|\zeta_k\rangle \to |\zeta_{k+J}\rangle$ goes off resonance as k increases and we expect limited photon production. We note that several methods to enhance photon generation have been proposed in similar setups, e.g., multitone modulations [21,39], time-varying modulation frequencies including effective Landau-Zener transitions [57], and optimum control strategies [58].

IV. DISCUSSION AND CONCLUSIONS

To confirm our analytic predictions we solve numerically the Schrödinger equation for Hamiltonian (1) considering the initial state $|\mathbf{0}, 0\rangle$ (which is approximately equal to the system's ground state in our regime of parameters) and feasible coupling constants $g_{0,1}/\omega = 5 \times 10^{-2}$, $g_{1,2}/\omega = 6 \times 10^{-2}$, and $g_{0,2}/\omega = 3 \times 10^{-2}$ (including all the CRTs, $c_{l,k} = 1$). For the sake of illustration we consider the sole modulation of E_2, setting $\varepsilon_1 = 0$ and $\varepsilon_2 = 7 \times 10^{-2}E_2^{(0)}$. In Fig. 1 we illustrate the three-photon DCE for the detunings $\Delta_1/\omega = 0.464$ and $\Delta_2/\omega = 0.106$ and modulation frequency $\eta/\omega = 3.0037$. We show the average photon number $n_{\rm ph} = \langle\hat{a}^\dagger\hat{a}\rangle$, Mandel's factor $Q = [\langle(\Delta\hat{n})^2\rangle - n_{\rm ph}]/n_{\rm ph}$ (which quantifies the spread of the photon number distribution, being $Q = 1 + 2n_{\rm ph}$ for the squeezed vacuum state), and the atomic populations $P_k = \langle\hat{\sigma}_{k,k}\rangle$. We also show the photon number distribution at the time instant $\omega t_* = 0.91 \times 10^5$ (when $n_{\rm ph}$ is maximum), confirming that the photon generation occurs via effective three-photon processes. We observe that for $t = t_*$

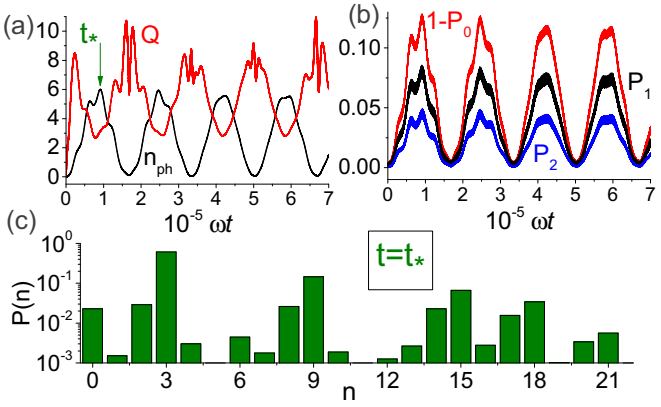

FIG. 1. System behavior for the three-photon DCE. (a) Dynamics of the average photon number $n_{\rm ph}$ and Mandel's Q factor. (b) Dynamics of the atomic populations: the probability that the atom leaves the initial state is $\lesssim$12%. (c) Photon statistics $P(n) = {\rm Tr}(\hat{\rho}|n\rangle\langle n|)$ for the time instant $\omega t_* = 0.91 \times 10^5$ [marked by the green arrow in (a)], where $\hat{\rho}$ is the total density operator. Note the local peaks at $n = 3k$, asserting the effective three-photon nature of the process.

the photon statistics does not show special behavior around $n \approx n_{\rm ph}$. The average photon number and the atomic populations exhibit a collapse-revival behavior due to increasingly off-resonant couplings between the probability amplitudes b_m in Eq. (3). Moreover, during the collapses $[n_{\rm ph}, (1 - P_0) \approx 0]$ Mandel's factor is very large, $Q \gg 1, n_{\rm ph}$, which is typical of *hyper-Poissonian* states that have long tails of distribution with very low (but not negligible) probabilities [38].

In Fig. 2 we perform a similar analysis for the one-photon DCE, setting the parameters $\Delta_1/\omega = 0.362$, $\Delta_2/\omega = 0.51$, and $\eta/\omega = 0.9978$. The qualitative behavior of $n_{\rm ph}$, Q, and the atomic populations is similar to that in the previous case, but the photon number distribution is completely different, as illustrated in Fig. 2(c) for $\omega t_* = 1.61 \times 10^5$. Now all the photon states are populated (as expected for an effective one-photon process), and the Q factor is always larger than $n_{\rm ph}$

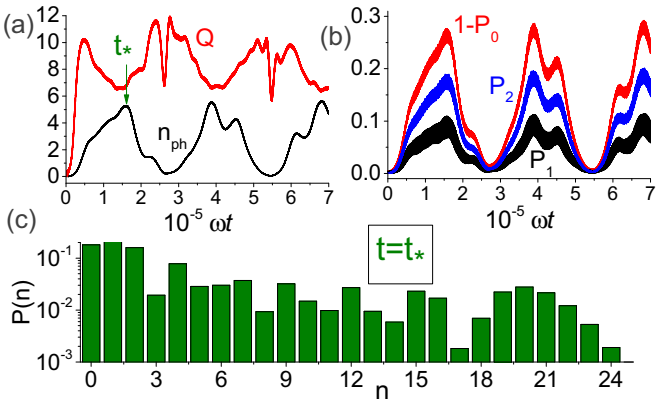

FIG. 2. System behavior for the one-photon DCE. Similar to Fig. 1. The probability that the atom leaves the initial state is now $\lesssim$30%. For $\omega t_* = 1.61 \times 10^5$ (c) the photon statistics lacks local peaks, indicating that the photons are generated via effective one-photon transitions.

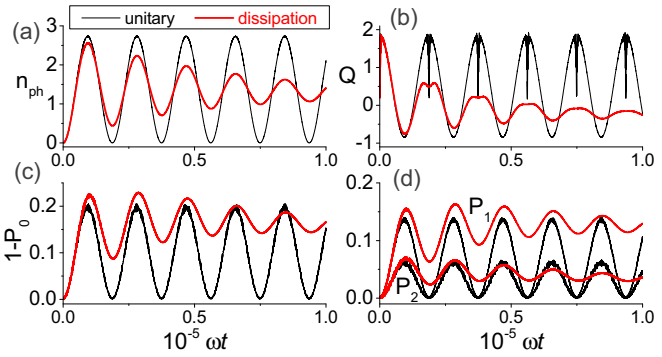

FIG. 3. Dissipative three-photon DCE. Behavior of $n_{\rm ph}$, Q, and P_k under unitary (thin black lines) and dissipative (thick red lines) evolutions. For initial times (till the first maximum of $n_{\rm ph}$) the effects of dissipation are small; for larger times the dissipation strongly affects the dynamics, but the main qualitative features persist.

due to the larger spread of the distribution. As in the previous example, there are no special features in the photon statistics for $n \approx n_{\rm ph}$, and one has similar probabilities of detecting any value ranging from 3 to 20 photons.

To assess the experimental feasibility of our proposal we solve numerically the phenomenological Markovian master equation for the density operator $\hat{\rho}$ [54,56],

$$\dot{\rho} = \frac{1}{i\hbar}[\hat{H}, \hat{\rho}] + \kappa\mathcal{L}[\hat{a}] + \sum_{k=0}^{1}\sum_{l>k}^{2}\gamma_{k,l}\mathcal{L}[\hat{\sigma}_{k,l}] + \sum_{k=1}^{2}\gamma_k^{(\phi)}\mathcal{L}[\hat{\sigma}_{k,k}],$$

where $\mathcal{L}[\hat{O}] \equiv \hat{O}\hat{\rho}\hat{O}^\dagger - \hat{O}^\dagger\hat{O}\hat{\rho}/2 - \hat{\rho}\hat{O}^\dagger\hat{O}/2$ is the Lindblad superoperator, κ is the cavity relaxation rate, and $\gamma_{k,l}$ ($\gamma_k^{(\phi)}$) are the atomic relaxation (pure dephasing) rates. Note that related works demonstrated that for $g_{k,l}/\omega < 10^{-1}$ and initial times this approach is a good approximation to a more rigorous microscopic model of dissipation [39,45,57]. Typical behavior of the three-photon DCE under unitary and dissipative evolutions is illustrated in Fig. 3, where we set $\Delta_1/\omega = 0.24$, $\Delta_2/\omega = -0.132$, $\eta/\omega = 3.0269$ [59] and feasible dissipative parameters $\gamma_{k,l} = \gamma_k^{(\phi)} = g_{0,1} \times 10^{-3}$ and $\kappa = g_{0,1} \times 10^{-4}$ (other parameters are as in Fig. 1). It is seen that for initial times the dissipative dynamics resembles the unitary one, indicating that our predictions could be verified in realistic circuit QED systems.

In conclusion, we have shown that for an artificial cyclic qutrit coupled to a single-mode cavity one can induce effective one- and three-photon transitions between the system's dressed states in which the atom remains approximately in the ground state. These effects occur in the dispersive regime of light-matter interaction for external modulation of some system parameter(s) with frequencies $\eta \approx \omega$ and $\eta \approx 3\omega$, respectively. We have evaluated the associated transition rates assuming the modulation of one or both excited energy levels of the atom, and our method can be easily extended to the perturbation of all the parameters in the Hamiltonian. For a constant modulation frequency the average photon number

and the atomic populations exhibit a collapse-revival behavior with a limited photon generation due to effective Kerr nonlinearities. The photon statistics is strikingly different from the standard (two-photon) DCE case, for which a squeezed vacuum state would be generated. Although we have focused on transitions that avoid exciting the atom, our approach can be applied to study of other uncommon transitions allowed by Δ atoms. Hence this study indicates viable alternatives for engineering effective interactions in nonstationary circuit QED using cyclic qutrits.

ACKNOWLEDGMENT

A.V.D. acknowledges partial support from Conselho Nacional de Desenvolvimento Científico e Tecnológico – CNPq.

APPENDIX: FULL EXPRESSIONS FOR THE DRESSED STATES

For the purpose of this paper it is sufficient to calculate the eigenstates of Hamiltonian $\hat{H}_0$ using the second-order perturbation theory. In the dispersive regime we obtain

$$
\begin{aligned}
|\zeta_k\rangle = \mathcal{N}_k\Bigg[& |\mathbf{0},k\rangle + \frac{g_{0,1}\sqrt{k}}{\Delta_1}|\mathbf{1},k-1\rangle - \frac{c_{0,1}g_{0,1}\sqrt{k+1}}{2\omega-\Delta_1}|\mathbf{1},k+1\rangle - \frac{g_{0,2}\sqrt{k}}{\omega-\Delta_3}|\mathbf{2},k-1\rangle - \frac{c_{0,2}g_{0,2}\sqrt{k+1}}{3\omega-\Delta_3}|\mathbf{2},k+1\rangle \\
& + \left(\frac{c_{0,1}g_{0,1}^2}{2\omega-\Delta_1} + \frac{c_{0,2}g_{0,2}^2}{3\omega-\Delta_3}\right)\frac{\sqrt{(k+1)(k+2)}}{2\omega}|\mathbf{0},k+2\rangle + \left(\frac{c_{0,1}g_{0,1}^2}{\Delta_1} - \frac{c_{0,2}g_{0,2}^2}{\omega-\Delta_3}\right)\frac{\sqrt{k(k-1)}}{2\omega}|\mathbf{0},k-2\rangle \\
& + \left(\frac{c_{1,2}c_{0,2}(k+1)}{3\omega-\Delta_3} + \frac{k}{\omega-\Delta_3}\right)\frac{g_{1,2}g_{0,2}}{\omega-\Delta_1}|\mathbf{1},k\rangle + \left(\frac{c_{0,1}(k+1)}{2\omega-\Delta_1} - \frac{c_{1,2}k}{\Delta_1}\right)\frac{g_{0,1}g_{1,2}}{2\omega_0-\Delta_3}|\mathbf{2},k\rangle \\
& + \frac{c_{0,2}g_{1,2}g_{0,2}\sqrt{(k+1)(k+2)}}{(3\omega-\Delta_3)(3\omega-\Delta_1)}|\mathbf{1},k+2\rangle - \frac{c_{1,2}g_{1,2}g_{0,2}\sqrt{k(k-1)}}{(\omega-\Delta_3)(\omega_0+\Delta_1)}|\mathbf{1},k-2\rangle \\
& + \frac{c_{0,1}c_{1,2}g_{0,1}g_{1,2}\sqrt{(k+1)(k+2)}}{(2\omega_0-\Delta_1)(4\omega-\Delta_3)}|\mathbf{2},k+2\rangle + \frac{g_{0,1}g_{1,2}\sqrt{k(k-1)}}{\Delta_1\Delta_3}|\mathbf{2},k-2\rangle\Bigg],
\end{aligned}
\tag{A1}
$$

where $\mathcal{N}_k = 1 + O[(g_0/\Delta_1)^2]$ is the normalization constant, whose value does not appear in our final (lowest-order) expressions.

For the eigenenergy corresponding to state $|\zeta_k\rangle$ we need to use the fourth-order perturbation theory to account for the effective Kerr nonlinearity. We get

$$
\begin{aligned}
\Lambda_k &= \omega k + L_1(k) + L_2(k), \\
L_1(k) &\equiv (\delta_1 - \delta_2 - c_{0,1}\delta_3 - c_{0,2}\delta_4)k - (c_{0,1}\delta_3 + c_{0,2}\delta_4), \\
L_2(k) &\equiv [\delta_1\beta_1(k) - \delta_2\beta_2(k)]k - [c_{0,1}\delta_3\beta_3(k) + c_{0,2}\delta_4\beta_4(k)](k+1).
\end{aligned}
$$

We defined the shifts $\delta_1 = g_{0,1}^2/\Delta_1$, $\delta_2 = g_{0,2}^2/(\omega-\Delta_3)$, $\delta_3 = g_{0,1}^2/(2\omega-\Delta_1)$, $\delta_4 = g_{0,2}^2/(3\omega-\Delta_3)$, $\delta_5 = g_{1,2}^2/(2\omega-\Delta_3)$, $\delta_6 = g_{1,2}^2/(\omega-\Delta_1)$. Other dimensionless functions of k are defined as

$$
\begin{aligned}
\beta_1(k) &\equiv (\delta_1 - c_{0,2}\delta_2)\frac{c_{0,1}(k-1)}{2\omega} + \frac{g_{1,2}^2(k-1)}{\Delta_1\Delta_3} + c_{1,2}\delta_5\left(\frac{c_{0,1}(k+1)}{2\omega-\Delta_1} - \frac{k}{\Delta_1}\right) - \frac{L_1(k)}{\Delta_1}, \\
\beta_2(k) &\equiv (c_{0,1}\delta_1 - \delta_2)\frac{c_{0,2}(k-1)}{2\omega} - \frac{c_{1,2}g_{1,2}^2(k-1)}{(\omega-\Delta_3)(\omega+\Delta_1)} + \delta_6\left(\frac{c_{1,2}c_{0,2}(k+1)}{3\omega-\Delta_3} + \frac{k}{\omega-\Delta_3}\right) + \frac{L_1(k)}{\omega-\Delta_3}, \\
\beta_3(k) &\equiv (\delta_3 + c_{0,2}\delta_4)\frac{k+2}{2\omega} + \delta_5\left(\frac{(k+1)}{2\omega_0-\Delta_1} - \frac{c_{1,2}k}{\Delta_1}\right) + \frac{c_{1,2}g_{1,2}^2(k+2)}{(2\omega-\Delta_1)(4\omega-\Delta_3)} + \frac{L_1(k)}{2\omega-\Delta_1}, \\
\beta_4(k) &\equiv (c_{0,1}\delta_3 + \delta_4)\frac{k+2}{2\omega} + c_{1,2}\delta_6\left(\frac{c_{1,2}(k+1)}{3\omega-\Delta_3} + \frac{k}{\omega-\Delta_3}\right) + \frac{g_{1,2}^2(k+2)}{(3\omega-\Delta_3)(3\omega-\Delta_1)} + \frac{L_1(k)}{3\omega-\Delta_3}.
\end{aligned}
$$

[1] V. V. Dodonov, Nonstationary Casimir effect and analytical solutions for quantum fields in cavities with moving boundaries, in *Modern Nonlinear Optics. Advances in Chemical Physics Series, Vol. 119*, edited by M. W. Evans (Wiley, New York, 2001), part 1, pp. 309–394.

[2] V. V. Dodonov, Current status of the dynamical Casimir effect, Phys. Scripta **82**, 038105 (2010).

[3] J. R. Johansson, G. Johansson, C. M. Wilson, and F. Nori, Dynamical Casimir effect in superconducting microwave circuits, Phys. Rev. A **82**, 052509 (2010).

[4] P. D. Nation, J. R. Johansson, M. P. Blencowe, and F. Nori, Colloquium: Stimulating uncertainty: Amplifying the quantum vacuum with superconducting circuits, Rev. Mod. Phys. **84**, 1 (2012).

[5] P. D. Nation, J. Suh, and M. P. Blencowe, Ultrastrong optomechanics incorporating the dynamical Casimir effect, Phys. Rev. A **93**, 022510 (2016).

[6] V. Macrì, A. Ridolfo, O. Di Stefano, A. F. Kockum, F. Nori, and S. Savasta, Nonperturbative Dynamical Casimir Effect in Optomechanical Systems: Vacuum Casimir-Rabi Splittings, Phys. Rev. X **8**, 011031 (2018).

[7] V. V. Dodonov and A. B. Klimov, Long-time asymptotics of a quantized electromagnetic field in a resonator with oscillating boundary, Phys. Lett. A **167**, 309 (1992).

[8] V. V. Dodonov, A. B. Klimov, and D. E. Nikonov, Quantum phenomena in nonstationary media, Phys. Rev. A **47**, 4422 (1993).

[9] C. K. Law, Effective Hamiltonian for the radiation in a cavity with a moving mirror and a time-varying dielectric medium, Phys. Rev. A **49**, 433 (1994).

[10] A. Lambrecht, M.-T. Jaekel, and S. Reynaud, Motion Induced Radiation from a Vibrating Cavity, Phys. Rev. Lett. **77**, 615 (1996).

[11] J.-Y. Ji, H.-H. Jung, J.-W. Park, and K.-S. Soh, Production of photons by the parametric resonance in the dynamical Casimir effect, Phys. Rev. A **56**, 4440 (1997).

[12] D. F. Mundarain and P. A. M. Neto, Quantum radiation in a plane cavity with moving mirrors, Phys. Rev. A **57**, 1379 (1998).

[13] N. Trautmann and P. Hauke, Quantum simulation of the dynamical Casimir effect with trapped ions, New J. Phys. **18**, 043029 (2016).

[14] A. Motazedifard, M. H. Naderi, and R. Roknizadeh, Dynamical Casimir effect of phonon excitation in the dispersive regime of cavity optomechanics, J. Opt. Soc. Am. B **34**, 642 (2017).

[15] V. V. Dodonov and J. T. Mendonça, Dynamical Casimir effect in ultra-cold matter with a time-dependent effective charge, Phys. Scripta T **160**, 014008 (2014).

[16] I. Carusotto, R. Balbinot, A. Fabbri, and A. Recati, Density correlations and analog dynamical Casimir emission of Bogoliubov phonons in modulated atomic Bose-Einstein condensates, Eur. Phys. J. D **56**, 391 (2010).

[17] J. C. Jaskula, G. B. Partridge, M. Bonneau, R. Lopes, J. Ruaudel, D. Boiron, and C. I. Westbrook, Acoustic Analog to the Dynamical Casimir Effect in a Bose-Einstein Condensate, Phys. Rev. Lett. **109**, 220401 (2012).

[18] V. V. Dodonov, Photon creation and excitation of a detector in a cavity with a resonantly vibrating wall, Phys. Lett. A **207**, 126 (1995).

[19] A. V. Dodonov, E. V. Dodonov, and V. V. Dodonov, Photon generation from vacuum in nondegenerate cavities with regular and random periodic displacements of boundaries, Phys. Lett. A **317**, 378 (2003).

[20] P. Lähteenmäki, G. S. Paraoanu, J. Hassel, and P. J. Hakonen, Dynamical Casimir effect in a Josephson metamaterial, Proc. Natl. Acad. Sci. USA **110**, 4234 (2013).

[21] A. V. Dodonov, Photon creation from vacuum and interactions engineering in nonstationary circuit QED, J. Phys.: Conf. Ser. **161**, 012029 (2009).

[22] S. De Liberato, D. Gerace, I. Carusotto, and C. Ciuti, Extracavity quantum vacuum radiation from a single qubit, Phys. Rev. A **80**, 053810 (2009).

[23] T. Fujii, S. Matsuo, N. Hatakenaka, S. Kurihara, and A. Zeilinger, Quantum circuit analog of the dynamical Casimir effect, Phys. Rev. B **84**, 174521 (2011).

[24] A. V. Dodonov, Analytical description of nonstationary circuit QED in the dressed-states basis, J. Phys. A **47**, 285303 (2014).

[25] J. Q. You and F. Nori, Atomic physics and quantum optics using superconducting circuits, Nature (London) **474**, 589 (2011).

[26] M. H. Devoret and R. J. Schoelkopf, Superconducting circuits for quantum information: An outlook, Science **339**, 1169 (2013).

[27] G. Wendin, Quantum information processing with superconducting circuits: A review, Rep. Prog. Phys. **80**, 106001 (2017).

[28] X. Gu, A. F. Kockum, A. Miranowicz, Y.-X. Liu, and F. Nori, Microwave photonics with superconducting quantum circuits, Phys. Rep. **718–719**, 1 (2017).

[29] J. Majer, J. M. Chow, J. M. Gambetta, J. Koch, B. R. Johnson, J. A. Schreier, L. Frunzio, D. I. Schuster, A. A. Houck, A. Wallraff, A. Blais, M. H. Devoret, S. M. Girvin, and R. J. Schoelkopf, Coupling superconducting qubits via a cavity bus, Nature **449**, 443 (2007).

[30] M. Hofheinz, H. Wang, M. Ansmann, R. C. Bialczak, E. Lucero, M. Neeley, A. D. O'Connell, D. Sank, J. Wenner, J. M. Martinis, and A. N. Cleland, Synthesizing arbitrary quantum states in a superconducting resonator, Nature **459**, 546 (2009).

[31] L. DiCarlo, J. M. Chow, J. M. Gambetta, L. S. Bishop, B. R. Johnson, D. I. Schuster, J. Majer, A. Blais, L. Frunzio, S. M. Girvin, and R. J. Schoelkopf, Demonstration of two-qubit algorithms with a superconducting quantum processor, Nature **460**, 240 (2009).

[32] J. Li, M. P. Silveri, K. S. Kumar, J.-M. Pirkkalainen, A. Vepsäläinen, W. C. Chien, J. Tuorila, M. A. Sillanpää, P. J. Hakonen, E. V. Thuneberg, and G. S. Paraoanu, Motional averaging in a superconducting qubit, Nat. Commun. **4**, 1420 (2013).

[33] S. J. Srinivasan, A. J. Hoffman, J. M. Gambetta, and A. A. Houck, Tunable Coupling in Circuit Quantum Electrodynamics Using a Superconducting Charge Qubit with a V-Shaped Energy Level Diagram, Phys. Rev. Lett. **106**, 083601 (2011).

[34] Y. Chen, C. Neill, P. Roushan, N. Leung, M. Fang, R. Barends, J. Kelly, B. Campbell, Z. Chen, B. Chiaro, A. Dunsworth, E. Jeffrey, A. Megrant, J. Y. Mutus, P. J. J. O'Malley, C. M. Quintana, D. Sank, A. Vainsencher, J. Wenner, T. C. White, M. R. Geller, A. N. Cleland, and J. M. Martinis, Qubit Architecture with High Coherence and Fast Tunable Coupling, Phys. Rev. Lett. **113**, 220502 (2014).

[35] S. Zeytinoğlu, M. Pechal, S. Berger, A. A. Abdumalikov Jr., A. Wallraff, and S. Filipp, Microwave-induced amplitude- and phase-tunable qubit-resonator coupling in circuit quantum electrodynamics, Phys. Rev. A **91**, 043846 (2015).

[36] I. M. de Sousa and A. V. Dodonov, Microscopic toy model for the cavity dynamical Casimir effect, J. Phys. A **48**, 245302 (2015).

[37] E. L. S. Silva and A. V. Dodonov, Analytical comparison of the first- and second-order resonances for implementation of the dynamical Casimir effect in nonstationary circuit QED, J. Phys. A **49**, 495304 (2016).

[38] A. V. Dodonov and V. V. Dodonov, Strong modifications of the field statistics in the cavity dynamical Casimir effect due to the

interaction with two-level atoms and detectors, Phys. Lett. A **375**, 4261 (2011).

[39] D. S. Veloso and A. V. Dodonov, Prospects for observing dynamical and antidynamical Casimir effects in circuit QED due to fast modulation of qubit parameters, J. Phys. B **48**, 165503 (2015).

[40] J. D. Strand, M. Ware, F. Beaudoin, T. A. Ohki, B. R. Johnson, A. Blais, and B. L. T. Plourde, First-order sideband transitions with flux-driven asymmetric transmon qubits, Phys. Rev. B **87**, 220505(R) (2013).

[41] Y. Lu, S. Chakram, N. Leung, N. Earnest, R. K. Naik, Z. Huang, P. Groszkowski, E. Kapit, J. Koch, and D. I. Schuster, Universal Stabilization of a Parametrically Coupled Qubit, Phys. Rev. Lett. **119**, 150502 (2017).

[42] Z. Chen, Y. Wang, T. Li, L. Tian, Y. Qiu, K. Inomata, F. Yoshihara, S. Han, F. Nori, J. S. Tsai, and J. Q. You, Single-photon-driven high-order sideband transitions in an ultrastrongly coupled circuit-quantum-electrodynamics system, Phys. Rev. A **96**, 012325 (2017).

[43] L. C. Monteiro and A. V. Dodonov, Anti-dynamical Casimir effect with an ensemble of qubits, Phys. Lett. A **380**, 1542 (2016).

[44] A. V. Dodonov, J. J. Díaz-Guevara, A. Napoli, and B. Militello, Speeding up the antidynamical Casimir effect with nonstationary qutrits, Phys. Rev. A **96**, 032509 (2017).

[45] A. V. Dodonov, D. Valente, and T. Werlang, Antidynamical Casimir effect as a resource for work extraction, Phys. Rev. A **96**, 012501 (2017).

[46] J. Casanova, R. Puebla, H. Moya-Cessa, and M. B. Plenio, Equivalence among generalized *n*th order quantum Rabi models, arXiv:1709.02714.

[47] S. Felicetti, M. Sanz, L. Lamata, G. Romero, G. Johansson, P. Delsing, and E. Solano, Dynamical Casimir Effect Entangles Artificial Atoms, Phys. Rev. Lett. **113**, 093602 (2014).

[48] D. Z. Rossatto, S. Felicetti, H. Eneriz, E. Rico, M. Sanz, and E. Solano, Entangling polaritons via dynamical Casimir effect in circuit quantum electrodynamics, Phys. Rev. B **93**, 094514 (2016).

[49] S. Felicetti, C. Sabín, I. Fuentes, L. Lamata, G. Romero, and E. Solano, Relativistic motion with superconducting qubits, Phys. Rev. B **92**, 064501 (2015).

[50] C. Sabín, B. Peropadre, L. Lamata, and E. Solano, Simulating superluminal physics with superconducting circuit technology, Phys. Rev. A **96**, 032121 (2017).

[51] N. B. Narozhny, A. M. Fedotov, and Yu. E. Lozovik, Dynamical Lamb effect versus dynamical Casimir effect, Phys. Rev. A **64**, 053807 (2001).

[52] D. S. Shapiro, A. A. Zhukov, W. V. Pogosov, and Yu. E. Lozovik, Dynamical Lamb effect in a tunable superconducting qubit-cavity system, Phys. Rev. A **91**, 063814 (2015).

[53] Y.-X. Liu, J. Q. You, L. F. Wei, C. P. Sun, and F. Nori, Optical selection rules and phase-dependent adiabatic state control in a superconducting quantum circuit, Phys. Rev. Lett. **95**, 087001 (2005).

[54] Y.-X. Liu, H.-C. Sun, Z. H. Peng, A. Miranowicz, J. S. Tsai, and F. Nori, Controllable microwave three-wave mixing via a single three-level superconducting quantum circuit, Sci. Rep. **4**, 7289 (2014).

[55] Y.-J. Zhao, J.-H. Ding, Z. H. Peng, and Y.-X. Liu, Realization of microwave amplification, attenuation, and frequency conversion using a single three-level superconducting quantum circuit, Phys. Rev. A **95**, 043806 (2017).

[56] P. Zhao, X. Tan, H. Yu, S.-L. Zhu, and Y. Yu, Circuit QED with qutrits: Coupling three or more atoms via virtual-photon exchange, Phys. Rev. A **96**, 043833 (2017).

[57] A. V. Dodonov, B. Militello, A. Napoli, and A. Messina, Effective Landau-Zener transitions in the circuit dynamical Casimir effect with time-varying modulation frequency, Phys. Rev. A **93**, 052505 (2016).

[58] F. Hoeb, F. Angaroni, J. Zoller, T. Calarco, G. Strini, S. Montangero, and G. Benenti, Amplification of the parametric dynamical Casimir effect via optimal control, Phys. Rev. A **96**, 033851 (2017).

[59] For these parameters n_{ph} is smaller than in Fig. 1, so the master equation can be solved numerically by truncating the Fock space at a smaller number of photons.